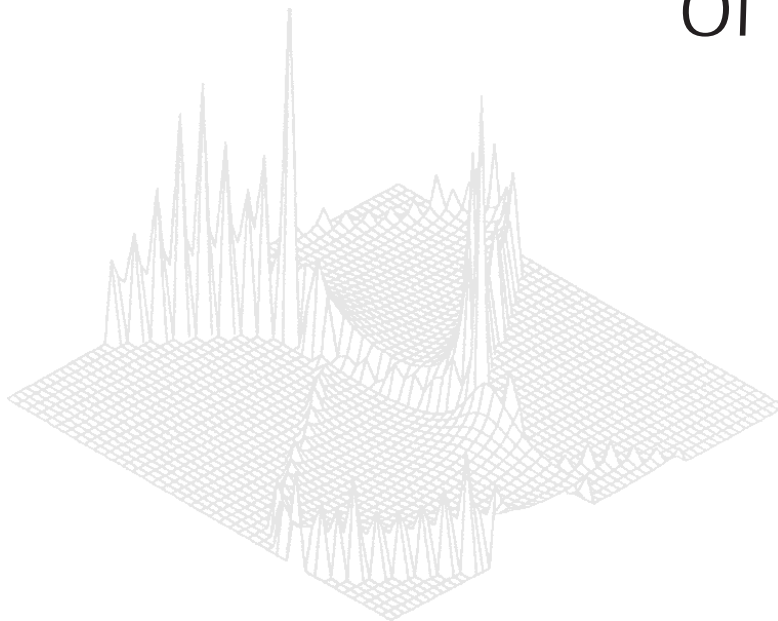

C S I R O P U B L I S H I N G

Australian Journal of Physics

Volume 51, 1998
© CSIRO 1998



A journal for the publication of
original research in all branches of physics

www.publish.csiro.au/journals/ajp

All enquiries and manuscripts should be directed to

Australian Journal of Physics

CSIRO PUBLISHING

PO Box 1139 (150 Oxford St)

Collingwood

Vic. 3066

Australia

Telephone: 61 3 9662 7626

Facsimile: 61 3 9662 7611

Email: peter.robertson@publish.csiro.au



Published by **CSIRO PUBLISHING**
for CSIRO and the
Australian Academy of Science



Dependence of ^{57}Fe Hyperfine Field in Yttrium Iron Garnet on Ionic Radius of Diamagnetic Defects: NMR Study*

H. Štěpánková,^{A,D} J. Kohout,^A P. Novák,^B J. Englisch,^A E.-G. Caspary^A
and H. Lütgemeier^C

^A Faculty of Mathematics and Physics, Charles University,
V Holešovičkách 2, CZ-180 00 Prague 8, Czech Republic.

^B Institute of Physics, Academy of Sciences, Prague, Czech Republic.

^C IFF, Forschungszentrum Jülich, Germany.

^D Corresponding author: Department of Low Temperature Physics,
Faculty of Mathematics and Physics, Charles University, V Holešovičkách 2,
CZ-180 00 Prague 8, Czech Republic.
email: stepanko@mbox.troja.mff.cuni.cz

Abstract

Satellite structure in ^{57}Fe NMR spectra of In^{3+} , Sc^{3+} , Ga^{3+} and Al^{3+} substituted yttrium iron garnets (YIG) was analysed taking into account results previously obtained for ‘antisite’ defects (Y^{3+} ions on Fe^{3+} sites) in nominally pure YIG. The influences of the diamagnetic substitution on the hyperfine field at the neighbouring iron nuclei were found to be remarkably dependent on the ionic radius of the substituent. In the case of two substituents in the vicinity of the resonating iron, an additivity of their effects within a 15% tolerance interval was verified.

1. Introduction

The hyperfine nuclear methods are capable of providing unique information on the local properties of magnetic materials, not available by most of the ‘standard’ methods characterising the sample as a whole. The hyperfine field on the iron nucleus in magnetic oxides is modified mainly by covalence effects, but electron supertransfer via oxygen ions plays an important role too (van der Woude and Sawatzky 1971). From the viewpoint of the dependence on the magnetisation direction, the supertransfer contribution consists of isotropic and anisotropic parts. While the former is associated with the s-electrons, the latter reflects the occupation of the 3d-electron states and therefore is closely related to the exchange interaction (Tomáš *et al.* 1995).

A diamagnetic substitution in the vicinity of the resonating ^{57}Fe nucleus alters its NMR frequency causing the appearance of a satellite line in the NMR spectrum. The frequency shift of the satellite corresponds in the first approximation to the contribution of the original iron ion to the local magnetic field at the resonating nucleus. A study of the satellite structure of NMR spectra caused by diamagnetic defects can thus provide information on individual iron–iron pair interactions. However, a certain dependence on the electron structure of the substituent is to be expected. A knowledge of the impact of the particular diamagnetic defect

* Refereed paper based on a contribution to the International Workshop on Nuclear Methods in Magnetism, held in Canberra on 21–23 July 1997.

(given by the position and type of a diamagnetic ion) on the NMR spectrum may then be, moreover, applied to detect the presence and the distribution of the impurities in the garnet in question.

Even if the diamagnetic ions, which are substituted instead of Fe^{3+} or Y^{3+} ions, have the same valence state and similar chemical bonding, the change of the hyperfine field depends on their ionic radius. The reason is that the ionic radius not only determines the local deformation associated with the substitution, but it also reflects the spatial distribution of the valence electrons and therefore the most important electron transfers. The linear dependence of the hyperfine field on the ionic radius was verified for the case when a Y^{3+} ion is substituted by a trivalent rare earth (English *et al.* 1994). On the other hand we found that Bi^{3+} and La^{3+} ions (differing in the electron structure) on the c sublattice of YIG cause quite a different change in the hyperfine field (Novák *et al.* 1988), despite their almost identical ionic radii.

Satellite structure of the ^{57}Fe NMR spectra has been measured for Ga^{3+} , Al^{3+} and In^{3+} substituted yttrium iron garnets (YIG) and interpreted using a simple superposition model (English *et al.* 1985; Brabenec *et al.* 1987). Only during the past few years, however, has substantially increased sensitivity, thanks to the pulse technique with coherent data summation and subsequent Fourier transform, brought about an improvement of the method sufficient to detect weak satellite lines of YIG with very low concentration of substituting ions or impurity defects (Wagner *et al.* 1995). The satellites resolved in the NMR spectrum of highly pure YIG with ‘antisite’ defects (Y^{3+} ions appear on the a sites normally occupied by the Fe^{3+} ions) were assigned (Novák *et al.* 1995) to several sets corresponding to various arrangements of the nearby antisite defect with respect to the resonating ^{57}Fe nucleus. The anisotropy tensors for the individual arrangements were determined analysing the dependence of the NMR spectrum on the direction of an external magnetic field applied in the (110) plane (Kohout *et al.* 1997; Štěpánková *et al.* 1998).

In the present work, NMR spectra of In^{3+} , Sc^{3+} , Ga^{3+} and Al^{3+} substituted YIG are analysed taking into account the ‘antisite’ results. The isotropic and anisotropic contributions to the resonance frequency shift are determined and compared. The dependence on the ionic radius is deduced and the validity of the superposition rule is discussed.

2. YIG Structure and Symmetry Considerations

The space symmetry group O_h^{10} of the yttrium iron garnet ($\text{Y}_3\text{Fe}_5\text{O}_{12}$) contains 96 symmetry operations per unit cell (International Tables 1952; Winkler 1981). The isomorphic point symmetry group is O_h with 48 operations. Sixteen crystallographically equivalent octahedral a sites with S_6 symmetry and 24 crystallographically equivalent tetrahedral d sites with S_4 symmetry are occupied by Fe^{3+} ions.

The ‘microscopic’ part of the local magnetic field \mathbf{B} at the resonating ^{57}Fe nucleus in zero external field results from the hyperfine field \mathbf{B}_{hf} , the Lorentz field \mathbf{B}_{L} and the dipolar field \mathbf{B}_{dip} (from magnetic dipoles inside Lorentz sphere) contributions:

$$\mathbf{B} = \mathbf{B}_{\text{hf}} + \mathbf{B}_{\text{dip}} + \mathbf{B}_{\text{L}}. \quad (1)$$

The values of \mathbf{B}_{hf} and \mathbf{B}_{dip} (and therefore that of \mathbf{B}) depend on the magnetisation direction. The NMR frequency f of a ^{57}Fe nucleus is proportional to the value of \mathbf{B} at its position by a factor $\gamma = 1.377 \text{ MHz T}^{-1}$. It may be expressed as a sum of an isotropic part I and an anisotropic part given by an anisotropy tensor \mathbf{A} and the magnetisation direction \mathbf{n} :

$$f = I + \sum_{i=1,j=1}^{3,3} n_i A_{ij} n_j. \quad (2)$$

The anisotropy tensor \mathbf{A} is a symmetrical second order traceless tensor and thus it includes five independent components in the general case. The resonance frequencies of the ^{57}Fe in the other crystallographically equivalent configurations are given by

$$\begin{aligned} f^s &= I + \sum_{i=1,j=1}^{3,3} n_i A_{ij}^s n_j \\ &= I + \sum_{i=1,j=1}^{3,3} \sum_{n=1,m=1}^{3,3} n_i (G^s)_{in}^{-1} A_{nm} G_{mj}^s n_j, \end{aligned} \quad (3)$$

where \mathbf{G}^s is the matrix of the vector representation (F_1) of the point symmetry operation, isomorphic with the space symmetry operation transforming the reference configuration to the configuration s . Because of the invariance of the anisotropy tensor with respect to the inversion, the number of different anisotropy tensors is 24 when the configurations have no symmetry left. This number is further reduced in the cases when the configurations possess some symmetry. The relevant forms of the anisotropy tensor and non-redundant symmetry operations are given in Table 1.

The experimental results presented in this work were obtained in a zero external magnetic field. The magnetisation is parallel to the easy direction $\langle 111 \rangle$ in this case. It means that in individual domains the magnetisation is along one of the directions $\pm[1, 1, 1]$, $\pm[-1, 1, 1]$, $\pm[1, -1, 1]$ or $\pm[-1, -1, 1]$. These directions are connected by fourfold rotations and inversion operations that are elements of the O_h point symmetry group. The alteration of the magnetisation direction then permutes the assignments between crystallographic configurations and NMR lines, but does not influence the resulting NMR spectrum (see Table 1). That is why only the $[1, 1, 1]$ magnetisation direction will be further considered.

The number of main (parent) lines in the zero external field NMR spectrum can be deduced from Table 1 for the case of no defects in the YIG structure, when the \mathbf{d} and the \mathbf{a} sites possess S_4 and S_6 symmetry respectively. While the resonance frequencies of all twenty-four Fe^{3+} \mathbf{d} sites with S_4 symmetry are equal, the anisotropic contribution causes splitting between the resonance frequencies of four Fe^{3+} \mathbf{a}_1 sites with the local three-fold symmetry axis parallel to the magnetisation (anisotropic contribution $2q$), and the remaining twelve Fe^{3+} \mathbf{a}_2 sites with different orientations of the local three-fold symmetry axis and the magnetisation (anisotropic contribution $-2q/3$). Thus, the intensity ratio of the $\mathbf{d} : \mathbf{a}_1 : \mathbf{a}_2$ main lines is 6:1:3.

Table 1. Forms and symmetry of the anisotropy tensor in substituted YIG and its contribution to the NMR resonance frequency in zero external field

Reference site symmetry	Form of anisotropy tensor for reference site	Number of different anisotropy tensors	Non-redundant point symmetry operations	Anisotropic contribution to resonance frequency for spontaneous magnetisation direction			
				$\pm[1, 1, 1]$	$\pm[-1, 1, 1]$	$\pm[1, -1, 1]$	$\pm[-1, -1, 1]$
None	$\begin{Bmatrix} t & q & r \\ q & u & s \\ r & s & -t-u \end{Bmatrix}$	24	$E, C_2(1), C_2(3), C_2(5), C_3(c), C_3^2(c)$ $C_2(x), C_4(z), C_4^3(y), C_2(6), C_3^2(a), C_3^2(b)$ $C_2(y), C_4(x), C_4^3(z), C_2(4), C_3(a), C_3(d)$ $C_2(z), C_4(y), C_4^3(x), C_2(2), C_3(b), C_3^2(d)$	$2(q+r+s)/3$	$2(r-q-s)/3$	$2(s-q-r)/3$	$2(q-r-s)/3$
S_6 or C_3 [1, 1, 1]	$\begin{Bmatrix} 0 & q & q \\ q & 0 & q \\ q & q & 0 \end{Bmatrix}$	4	E $C_4(z)$ $C_4^3(z)$ $C_2(z)$	$2q$ $-2q/3$ $2q/3$ $-2q/3$	$-2q/3$ $-2q/3$ $2q$ $-2q/3$	$-2q/3$ $2q$ $-2q/3$ $-2q/3$	$-2q/3$ $-2q/3$ $-2q/3$ $2q$
S_4 [0, 0, 1]	$\begin{Bmatrix} t & 0 & 0 \\ 0 & t & 0 \\ 0 & 0 & -2t \end{Bmatrix}$	3	$E, C_3(c), C_3^2(c)$	0	0	0	0

Table 2. Specification of the configurations inducing appearance of the main and single satellite lines in YIG spectrum

Notation	Site of resonating nucleus	Site of diamagnetic substituent	Distance between substituent and res. nucleus (nm)	Number of cryst. equivalent subst. sites	Symmetry of configuration	Number of different aniz. tensors	Number of lines for magnetisation in [1, 1, 1]	Relative intensity of one line ^A
a_1	a_1	—	—	—	S_6	1	1	4
a_2	a_2	—	—	—	S_6	3	1	12
$a_1\{a^{1*}\}$	a_1	1st a vicinity of a	0.535	2	C_3	1	1	8 ξ
$a_2\{a^{1*}\}$	a_2	at C_3	—	—	C_3	3	1	24 ξ
$a_1\{a^1\}$	a_1	1st a vicinity of a	0.535	6	None	6	1	24 ξ
$a_2\{a^{1n}\}$	a_2	outside C_3	—	—	None	18	3	24 ξ
$a_1\{a^2\}$	a_1	2nd a vicinity of a	0.618	6	None	6	1	24 ξ
$a_2\{a^{2n}\}$	a_2	—	—	—	None	18	3	24 ξ
$a_1\{a^{5*}\}$	a_1	5th a vicinity of a	1.070	2	C_3	1	1	8 ξ
$a_2\{a^{5*}\}$	a_2	at C_3	—	—	C_3	3	1	24 ξ
$a_1\{d^1\}$	a_1	1st d vicinity of a	0.345	6	None	6	1	24 ξ
$a_2\{d^{1n}\}$	a_2	—	—	—	None	18	3	24 ξ
d	d	—	—	—	S_4	3	1	24
$d\{a^{Ii}\}$	d	1st a vicinity of d	0.345	4	None	24	4	24 ξ
$d\{a^{IIi}\}$	d	2nd a vicinity of d	0.557	4	None	24	4	24 ξ
$d\{d^{Ii}\}$	d	1st d vicinity of d	0.378	4	None	24	4	24 ξ

^A Relative to the reference intensity taken as 24, 4 and 12 for the d , a_1 and a_2 main lines respectively. Parameter ξ is defined by equation (4).

Diamagnetic substitution in the vicinity of the resonating nucleus modifies the values of both isotropic and anisotropic contributions and in general perturbs the symmetry of the anisotropy tensor. Each type of crystallographically equivalent configuration of the substituent and the resonating nucleus will then cause in principle the appearance of four satellite lines in the spectral region of both the **a** and **d** subspectra. Exceptions are the substitutions on positions lying on the local symmetry axis of the resonating iron, when the local symmetry is not destroyed completely. It is the case for the positions of the first and the fifth **a** neighbours of **a** sites lying on the local C_3 axis, when the number of satellite lines corresponding to the crystallographically equivalent configurations of the resonating nucleus and the substituent is the same as the number of the main lines.

Supposing a random distribution, the probability for a substitution on a certain position is given by the concentration c of the substituent and of the Fe^{3+} ions in the corresponding sublattice. If there are N crystallographically equivalent positions in a certain vicinity of the resonating nucleus and M different satellite lines are generated in the spectrum by single substitutions in this vicinity, the intensity ratio σ of a satellite line to its parent line is equal to

$$\sigma = \frac{N}{M}\xi, \quad \text{where} \quad \xi = \frac{c}{1-c}. \quad (4)$$

The relative intensities and notation used for single satellites observable in our spectra are given in Table 2.

If a random distribution of the substituent in a sublattice is expected, the probability of composite satellites caused by two or more substitutions in the vicinity of the resonating nucleus can be calculated as a product of a corresponding power of ξ and a number of combinations in occupation inducing the same satellite line. The relative intensities and notation used for double composite satellites relevant for our spectra are given in Table 3.

3. Experimental

The ^{57}Fe NMR spectra were carried out using a pulse NMR spectrometer with coherent data summation in the time domain and subsequent Fourier transform. The measured sample was placed either in the coil of the tuned resonant circuit, or the broadband probe was used with the sensitivity estimated to be approximately five times lower. Spin echoes excited either by conventional two pulse sequences or by Carr-Purcell pulse series were detected. The pulse lengths used were about 1–4 μs , with pulse separation 100–350 μs . The repetition period of a pulse sequence was chosen to be sufficiently longer than the value of the spin-lattice relaxation times of the individual sample. The amplitude of the rf field was carefully optimised to excite the NMR signal from nuclei inside magnetic domains only. The excitation frequency was successively changed through the spectra frequency region with a step of 30–50 kHz. At each excitation frequency the fast Fourier transform of NMR signal time dependence was performed and the individual Fourier transforms were overlapped to form a spectrum.

The basic measurements were performed at 4.2 K. The temperature dependences of NMR spectra were measured using a continuous flow helium cryostat. Nominally

pure single crystals of yttrium iron garnets (with antisite defects but containing a minimum of other defects or impurities) were prepared by two different techniques: growth from a BaO/B₂O₃ flux (concentration of Y³⁺ ions on *a* sites $c \sim 0.008$) and by a floating zone technique ($c \sim 0.014$). Polycrystalline samples with diamagnetic substitutions Y₃Fe_{5-x}Al_xO₁₂ ($x = 0.1$), Y₃Fe_{5-x}Ga_xO₁₂ ($x = 0.1$ and 0.2) and Y₃Fe_{5-x}In_xO₁₂ ($x = 0.08$) were prepared by ceramic technology (Winkler 1981). Single crystals of Y₃Fe_{5-x}Sc_xO₁₂ ($x = 0.2$ and 0.4) were grown from PbO/PbF₂/B₂O₃ flux.

4. Results and Discussion

NMR spectra of In³⁺, Sc³⁺, Al³⁺ and Ga³⁺ substituted YIG measured at 4.2 K in zero external field are shown in Figs 1–5. It is known (Winkler 1981) that In³⁺ and Sc³⁺ occupy *a* sites while Al³⁺ and Ga³⁺ (in low concentrations) enter predominately *d* sites. The resolved lines in In³⁺ and Sc³⁺ substituted YIG were assigned, where feasible by analogy with the spectrum corresponding to the ‘antisite’ defects interpreted previously (Novák *et al.* 1995) by using temperature dependences of the resonance frequencies. Variation of the satellite frequencies with the type of the diamagnetic substituent is remarkable. It can be seen for instance by comparing the $d\{a^I\}$ line frequencies in Figs 1 and 3, the $a_1\{a^1\}$ lines in Figs 2 and 4, or the $a_1\{d^1\}$ lines in Fig. 5, top and bottom.

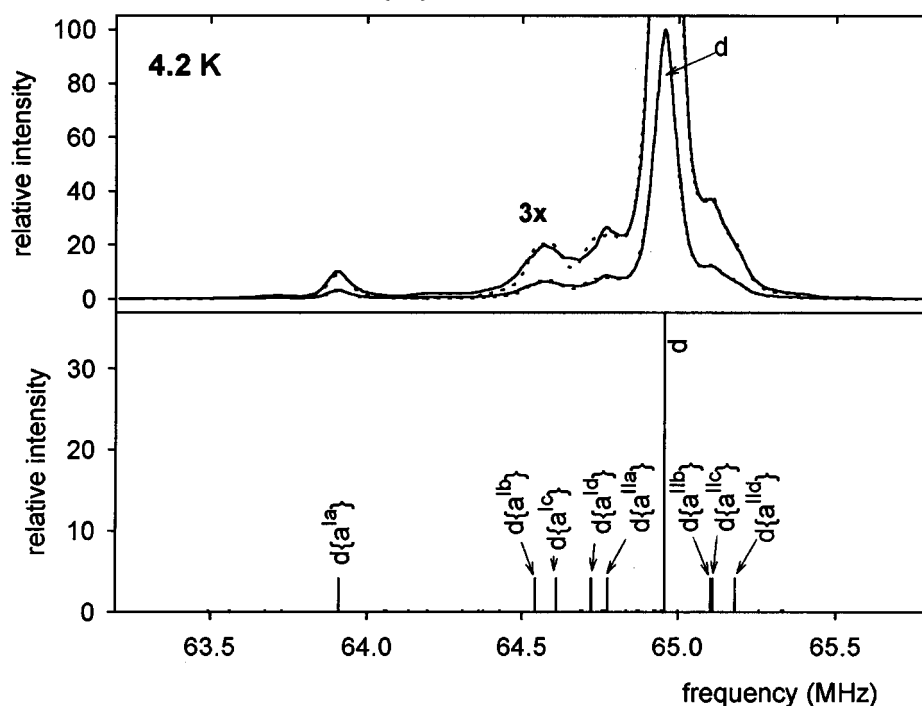


Fig. 1. ⁵⁷Fe NMR spectrum of In³⁺ substituted ($x = 0.08$) YIG in the region of the *d* site resonance frequency. Solid curve—experimental results, dotted curve—fitted spectral shape. (The dotted curve is mainly overlapped by the solid one, and therefore the spectrum magnified three times is also shown to make the differences visible.) *Bottom*: Composition of the satellite structure scheme of the resonance frequencies and relative intensities (notation according to Table 2).

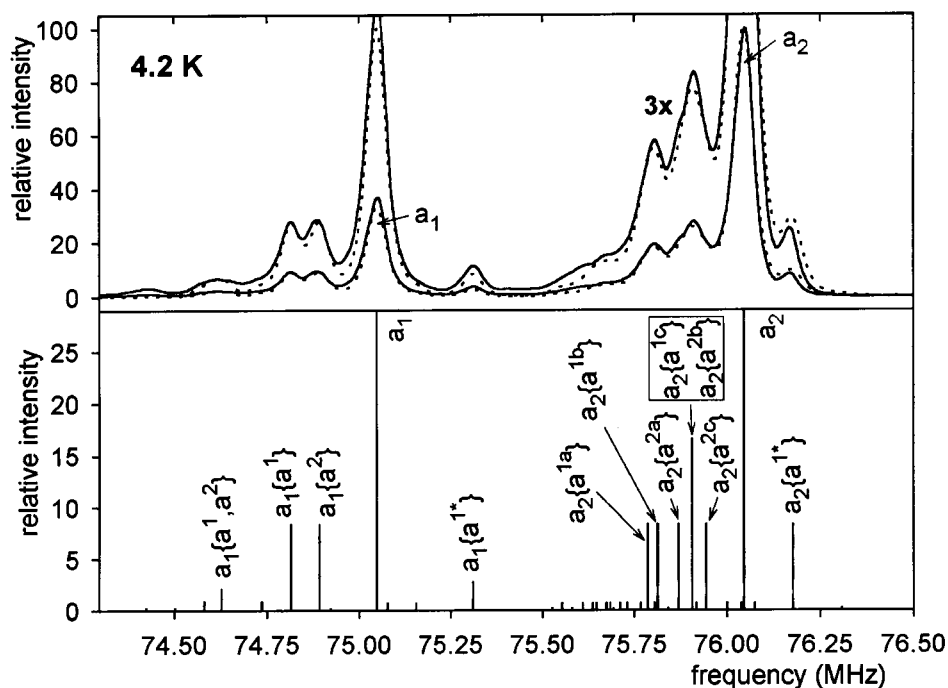


Fig. 2. ^{57}Fe NMR spectrum of In^{3+} substituted ($x = 0.08$) YIG in the region of the a site resonance frequency. Solid curve—experimental results, dotted curve—fitted spectral shape. Bottom: Composition of the satellite structure scheme of the resonance frequencies and relative intensities (notation according to Tables 2 and 3).

In order to find the positions of the unresolved satellite lines, the NMR spectra of In^{3+} and Sc^{3+} substituted samples were treated by a least squares fit to a set of lines of the same shape and halfwidth, with intensities corresponding to the relations given in Tables 2 and 3. A Pearson function with a shape coefficient close to 2 (extreme values obtained from the fit were 1.85 in the In^{3+} substituted sample and 2.4 for a lines in that substituted by Ga^{3+}) was found to provide the best agreement with the experimental lineshapes. Because of certain deviations of the composite satellite frequencies from the values given by the sum of the relevant single satellites shifts (expected by a superposition rule discussed below), the following procedure was used to fit the structure of the NMR spectra: First, the least-squares fit was completed supposing the additivity in positions of the composite satellite frequencies. Next, scaling factors were introduced to correct the positions of the multiple satellites where disagreement between the experimental and fitted spectra were obvious. Then, a new least-squares fit was carried out with use of the scale factors (not further optimised).

This procedure is possible because of the relative low intensity of composite satellites, so that the introduction of the scale factors influenced the spectrum only marginally. The fit provided a satisfactory agreement between the experimental and fitted spectra. The shifts obtained for the single satellite resonance frequencies from the corresponding main lines are listed in Tables 4 and 5. The plausibility of the single satellites resonance frequencies was carefully examined in the cases

when the satellite line was not resolved in the experimental spectrum. If the resonance frequency was not obtained unambiguously, with a standard deviation from the fit larger than 25 kHz, or did not correspond to any minimum in the second derivative of the spectrum, it was not accepted for further treatment.

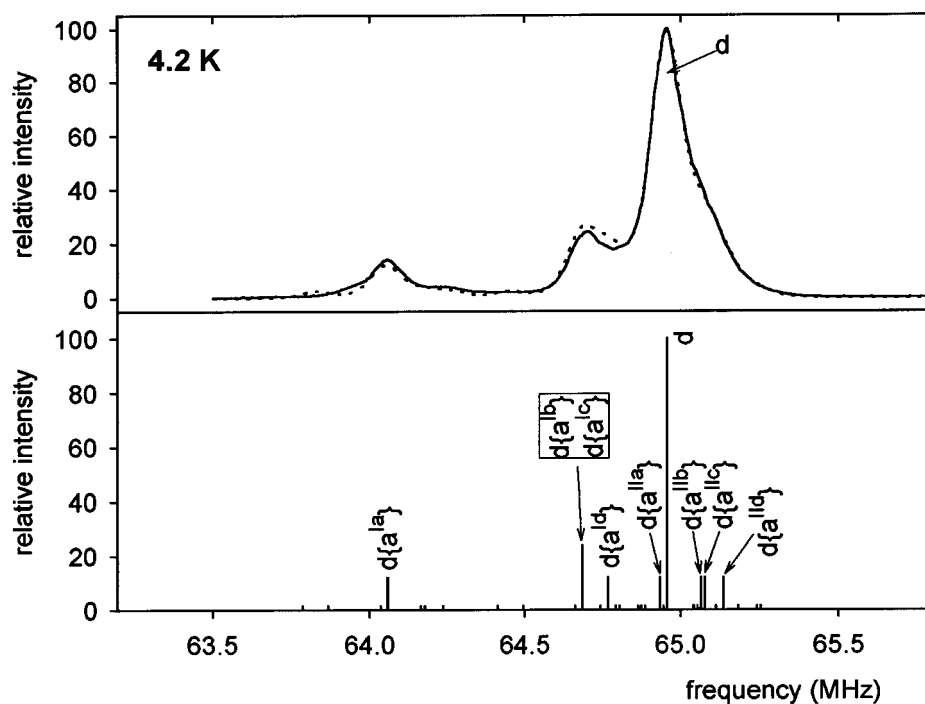


Fig. 3. ^{57}Fe NMR spectrum of Sc^{3+} substituted ($x = 0.2$) YIG in the region of the d site resonance frequency. Solid curve—experimental results, dotted curve—fitted spectral shape. *Bottom:* Composition of the satellite structure scheme of the resonance frequencies and relative intensities (notation according to Table 2).

The $a_2\{a^{1n}\}$ and $a_2\{a^{2n}\}$ satellites ($n = a, b, c$) in the In^{3+} substituted sample could not be assigned on the basis of the analogy with ‘antisite’ satellites only, because the differences between their frequencies are quite comparable with the changes caused by the dependence on the diamagnetic substituent. That is why the temperature dependence of the resonance frequencies was employed. As discussed by Novák *et al.* (1995), the resonance frequencies of the satellites corresponding to the crystallographically equivalent configurations of the resonating nucleus and the substituent are uniformly shifted with increased temperature. This can be seen most clearly from the plot of the temperature dependence of the differences between the satellite frequency (normalised to a low temperature value) and that of the corresponding (d or a_2) main line

$$\delta(T) = \frac{f^{\text{sat}}(T)}{f^{\text{sat}}(4.2 \text{ K})} - \frac{f^{\text{main}}(T)}{f^{\text{main}}(4.2 \text{ K})}, \quad (5)$$

as is shown in Fig. 6. The top part of Fig. 6 demonstrates similar behaviour of the satellites corresponding to the crystallographically equivalent configurations of the substitution and the resonating nucleus. From the bottom part of Fig. 6, the interpretation of the $a_2\{a^{1n}\}$ and $a_2\{a^{2n}\}$ satellites (shown in Fig. 2) was obtained.

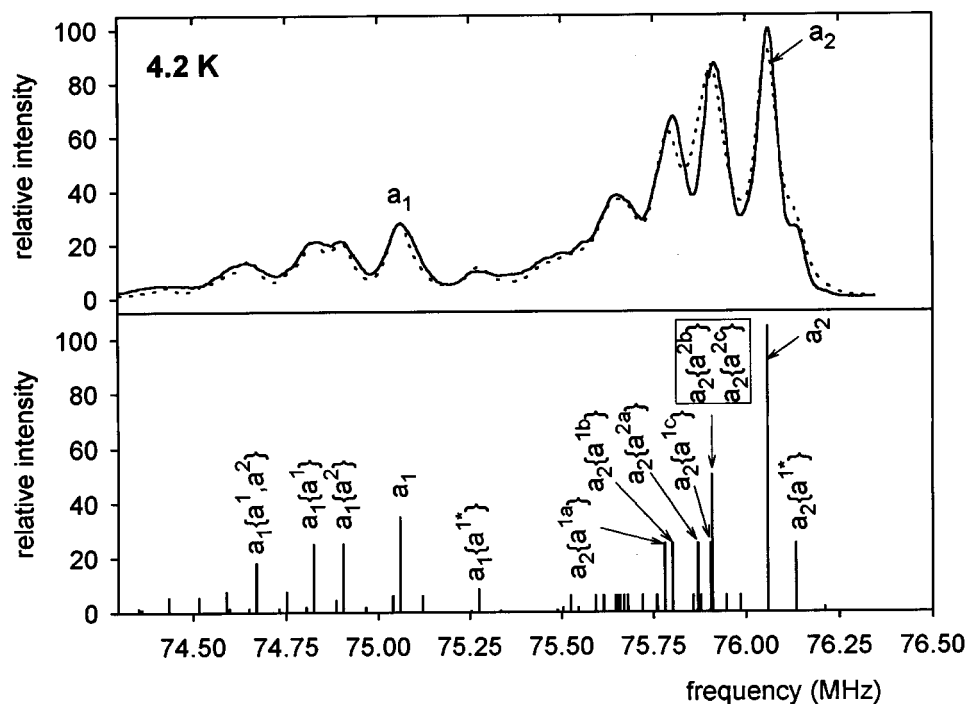


Fig. 4. ^{57}Fe NMR spectrum of Sc^{3+} substituted ($x = 0.2$) YIG in the region of the a site resonance frequency. Solid curve—experimental results, dotted curve—fitted spectral shape. Bottom: Composition of the satellite structure scheme of the resonance frequencies and relative intensities (notation according to Tables 2 and 3).

We shall attempt to interpret the satellite frequencies supposing the validity of a superposition rule. Following this rule, each cation in the vicinity contributes to the magnetic field on the resonating nucleus independently of occupation of the other cation sites. The frequency shift caused by a diamagnetic substitution of a Fe^{3+} ion can thus be understood as a measure of the local magnetic field modification induced by removing the Fe^{3+} contribution and by appearance of the contribution of the diamagnetic ion. In our experiments, the Fe^{3+} ion ($3d^5$ electron configuration) was replaced by an ion with closed outer shell [the electron configurations of the substituents are $2p^6$ (Al^{3+}), $3p^6$ (Sc^{3+}), $3d^{10}$ (Ga^{3+}), $4p^6$ (Y^{3+}) and $4d^{10}$ (In^{3+})].

Investigating the correlation of the single satellite shifts with the ionic radius for the three samples with the substitution on the a sites, an approximately linear dependence was found as illustrated in Fig. 7. The parameters α and β of the linear dependence defined by

$$\Delta f(R^{A^{3+}}) = \alpha(R^{A^{3+}} - R^{Fe^{3+}}) + \beta, \quad (6)$$

where R is the ionic radius, were determined by a linear regression (Tables 4 and 5). Here β represents values of the resonance frequency shift extrapolated to an ionic radius of the Fe^{3+} ion in a given site (0.0645 nm for an a site and 0.049 nm for a d site; Shannon 1976). It can be seen that for configurations when the substituent does not enter the nearest iron site connected with the resonating nucleus by the superexchange interaction in the $Fe^{3+}(\uparrow)-O^{2-}-Fe^{3+}(\downarrow)$ triad, the anisotropy part of the contribution is substantially reduced after extrapolation. It implies that in those cases the difference in the ionic radius induces remarkable changes in the hyperfine field anisotropy.

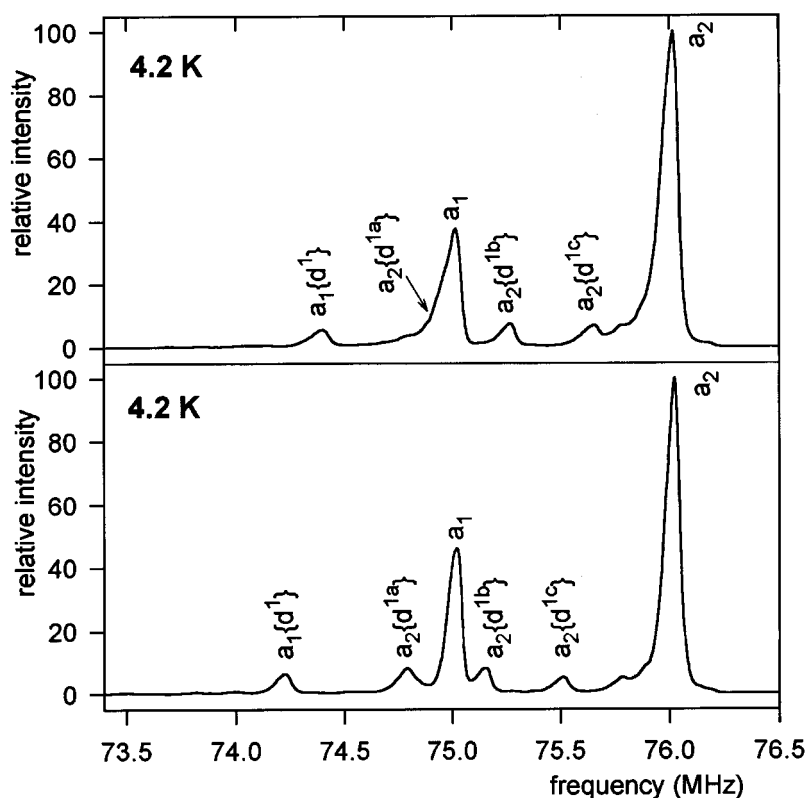


Fig. 5. ^{57}Fe NMR spectrum of Al^{3+} ($x = 0.1$) substituted (*top*) and of Ga^{3+} ($x = 0.1$) substituted YIG (*bottom*) in the region of the a site resonance frequency. The main and single satellite lines are assigned (notation according to Table 2).

When the frequency shifts of all satellites corresponding to a certain set of crystallographically equivalent configurations are known in a zero external field, it is possible to determine values of the isotropic term and of the non-diagonal elements of the anisotropy tensor according to the relations given in Table 1. The values obtained from the extrapolated frequency shifts to the Fe^{3+} ionic radius are listed in Table 6. They represent mainly the supertransfer contributions of

the given Fe^{3+} ion to the field at the resonating nucleus including the dipolar contribution. The parameters of the dipolar contribution can be easily calculated (results are also shown in Table 6), but because of an ambiguity in the substituent position for which the experimental data are obtained they cannot be directly subtracted. The exceptions are sets with the equal non-diagonal components of the dipolar contribution tensor [the case of the $a\{a^{1*}\}$ and $a\{a^2\}$ sets].

Table 3. Numbers and relative intensities of composite satellite lines

Notation ^A	Number of lines for magnetisation in [1, 1, 1]	Relative intensity of one line ^B
$a_1\{a^{1*}, a^{1*}\}$	1	$4\xi^2$
$a_1\{a^{1*}, a^1\}$	1	$48\xi^2$
$a_1\{a^{1*}, a^2\}$	1	$48\xi^2$
$a_1\{a^1, a^1\}$	1	$60\xi^2$
$a_1\{a^1, a^2\}$	1	$144\xi^2$
$a_1\{a^2, a^2\}$	1	$60\xi^2$
$a_2\{a^{1*}, a^{1*}\}$	1	$12\xi^2$
$a_2\{a^{1*}, a^{1n}\}$	3	$48\xi^2$
$a_2\{a^{1*}, a^{2n}\}$	3	$48\xi^2$
$a_2\{a^{1n}, a^{1n}\}$	3	$12\xi^2$
$a_2\{a^{1n}, a^{1m(\neq n)}\}$	3	$48\xi^2$
$a_2\{a^{1n}, a^{2m}\}$	9	$48\xi^2$
$a_2\{a^{2n}, a^{2m}\}$	3	$12\xi^2$
$a_2\{a^{1n}, a^{1m(\neq n)}\}$	3	$48\xi^2$
$d\{a^{Ii}, a^{Ij(\neq i)}\}$	6	$24\xi^2$
$d\{a^{IIi}, a^{IIj}\}$	16	$24\xi^2$
$d\{a^{IIIi}, a^{IIIj(\neq i)}\}$	6	$48\xi^2$
$a_1\{d^1, d^1\}$	1	$60\xi^2$
$a_2\{d^{1n}, d^{1n}\}$	3	$12\xi^2$
$a_2\{d^{1n}, d^{1m(\neq n)}\}$	3	$48\xi^2$

^A Indices n, m, i, j are used for convenience to resolve different lines in the spectrum: $n(m) = a, b, c$ and $i(j) = a, b, c, d$.

^B Relative to the reference intensity taken as 24, 4 and 12 for the d , a_1 and a_2 main lines respectively. Parameter ξ is defined by equation (4).

The superposition rule also implies that the shift of the ‘composite’ satellite, caused by two substitutions, should be equal to the sum of shifts caused by individual substitutions. Positions of several composite satellites, well resolved and unambiguously assigned in the spectra were used to check this additivity of frequency shifts. Fig. 8 shows (as an example) details of the spectra of YIG with ‘antisite’ defects and with Ga^{3+} substitution in comparison with the predicted spectrum of the composite satellites calculated from the structure of the main and single satellite lines according to the superposition rule. The agreement of the superposition rule with the experimentally obtained positions of the composite satellites was found to be better than 15%. Deviations from the superposition rule were characterised by scaling factors Φ , defined by

$$f^{\text{exp}} = \Phi f^{\text{addit}}, \quad (7)$$

and are listed in Table 7.

Table 4. Frequency shifts of single satellites from the parent lines for Y^{3+} , In^{3+} and Sc^{3+} substituents and coefficients of the frequency shift linear dependence on ionic radii

Satellite ^A	Y^{3+}	In^{3+}	Sc^{3+}	Linear coefficients ^C	
	$R = 0.09$ nm Δf (MHz) ^B	$R = 0.08$ nm Δf (MHz) ^B	$R = 0.0745$ nm Δf (MHz) ^B	α (MHz nm ⁻¹)	β (MHz)
$a_1\{a^{1*}\}$	0.356	0.263	0.215	9.17 ± 0.14	0.122 ± 0.010
$a_1\{a^1\}$	-0.229	-0.233	-0.235	0.39 ± 0.09	-0.239 ± 0.009
$a_1\{a^2\}$	-0.192	-0.165	-0.154	-2.54 ± 0.17	-0.127 ± 0.007
$a_2\{a^{1*}\}$	0.163	0.130	0.076	4.5 ± 1.3	0.051 ± 0.027
$a_2\{a^{1a}\}$	-0.258	-0.258	-0.278	0.8 ± 0.8	-0.278 ± 0.022
$a_2\{a^{1b}\}$	-0.240	-0.230	-0.278	1.1 ± 2.1	-0.267 ± 0.051
$a_2\{a^{1c}\}$	-0.087	-0.139	-0.19	5.8 ± 0.8	-0.235 ± 0.022
$a_2\{a^{2a}\}$	-0.228	-0.176	-0.15	-5.15 ± 0.09	-0.097 ± 0.020
$a_2\{a^{2b}\}$	-0.151	-0.139	-0.15	-0.7 ± 0.7	-0.134 ± 0.020
$a_2\{a^{2c}\}$	-0.138	-0.104	-0.11	-2.6 ± 0.9	-0.071 ± 0.035
$d\{a^{1a}\}$	-1.255	-1.048	-0.899	-22.7 ± 1.6	-0.68 ± 0.19
$d\{a^{1b}\}$	-0.578	-0.425	-0.272	-18.0 ± 2.5	-0.12 ± 0.06
$d\{a^{1c}\}$	-0.561	-0.357	-0.272	-19.3 ± 1.0	-0.07 ± 0.02
$d\{a^{1d}\}$	-0.531	-0.203	(-0.19)	-32.4 ± 2.4	0.29 ± 0.14
$d\{a^{1Ia}\}$	0.202	(0.00)	(-0.02)	—	—
$d\{a^{1Ib}\}$	0.244	0.147	0.107	9.3 ± 0.5	0.01 ± 0.08
$d\{a^{1Ic}\}$	0.267	0.154	0.119	10.5 ± 1.0	0.00 ± 0.15
$d\{a^{1Id}\}$	0.342	0.225	0.178	10.8 ± 0.8	0.06 ± 0.12

^A Notation according to Table 2.^B Satellite frequency minus the frequency of the corresponding parent line. Values of ionic radii R are taken from Shannon (1976). The frequency shifts in parentheses are less reliable (see text) and thus were not employed in the linear regression (Fig. 7).^C Linear coefficients defined by equation (6).**Table 5.** Frequency shifts of single satellites from the parent lines for Al^{3+} and Ga^{3+} substituents and coefficients of the frequency shift linear dependence on ionic radii

Notation ^A	Al^{3+}	Ga^{3+}	Linear coefficients ^C	
	$R = 0.039$ nm Δf (MHz) ^B	$R = 0.047$ nm Δf (MHz) ^B	α (MHz nm ⁻¹)	β (MHz)
$a_1\{d^1\}$	-0.620	-0.796	-22 ± 3	-0.84 ± 0.02
$a_2\{d^{1a}\}$	-1.215	-1.241	-3.2 ± 2.5	-1.25 ± 0.02
$a_2\{d^{1b}\}$	-0.752	-0.877	-16 ± 3	-0.91 ± 0.02
$a_2\{d^{1c}\}$	-0.361	-0.520	-20 ± 3	-0.56 ± 0.02

^A Notation according to Table 2.^B Satellite frequency minus the frequency of the corresponding parent line. Values of ionic radii R are taken from Shannon (1976).^C Linear coefficients defined by equation (6).

In the spectrum of the Ga^{3+} substituted sample (Fig. 8), the composite satellite $a_1\{a^1, a^1\}$ seems to be split. This phenomenon is probably caused by the fact, that several different crystallographically non-equivalent configurations of the resonating iron and two substituting ions are possible in this case, and the deviations from the superposition rule then remove the degeneracy of their frequency shifts.

5. Conclusions

Our results prove that the effect of the diamagnetic substitution on the hyperfine field at neighbouring iron nuclei depends remarkably on the ionic radius

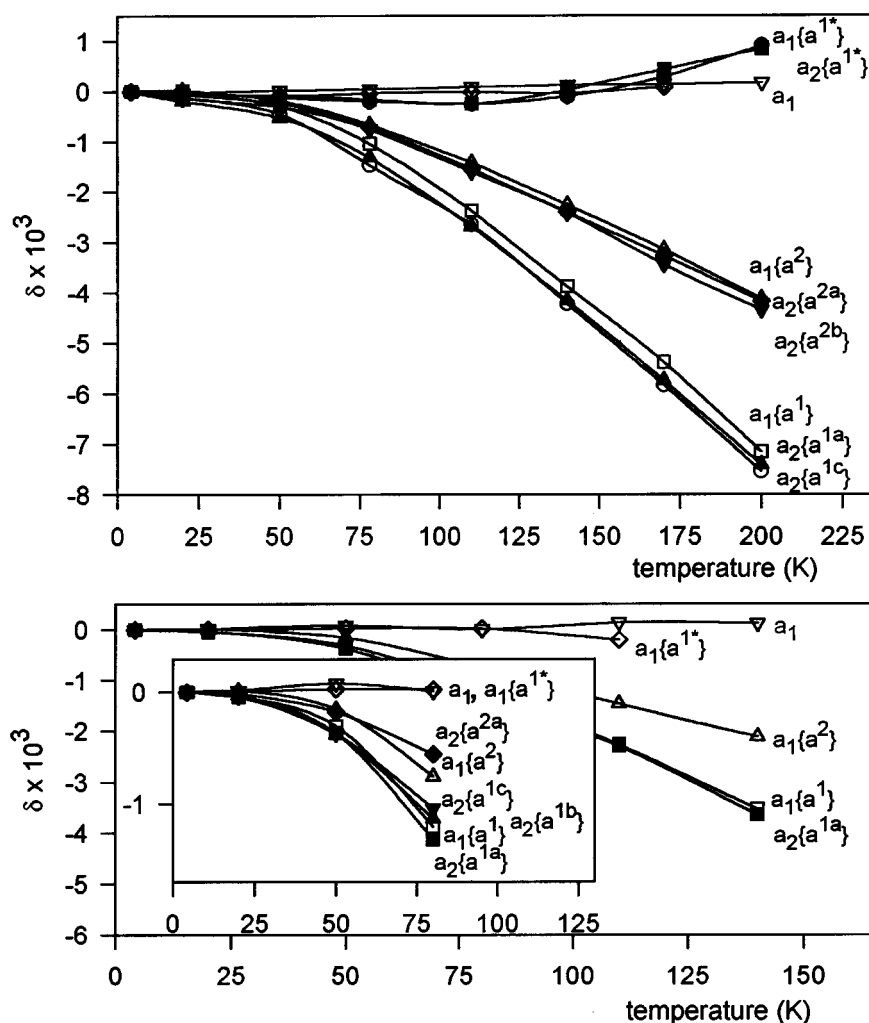


Fig. 6. Temperature dependence of the relative frequency shift δ of satellite lines caused by 'antisite' defects (Y^{3+} on a sites, $x = 0.014$) (top) and in In^{3+} ($x = 0.08$) substituted YIG (bottom). The parameter δ is defined by equation (5).

of the substituent. The approximate additivity of the effects in the case of a simultaneous influence of two substituents and the approximate linearity of the dependence on the ionic radius were found. Changes in the isotropic part and in the non-diagonal elements of the anisotropy tensor of the hyperfine field caused by diamagnetic substitution in the vicinity of the resonating iron nucleus were extrapolated for a zero difference in ionic radius between the substituent and substituted Fe^{3+} ion. These values (Table 6) are believed to estimate the individual contributions of the replaced iron ions, useful for future development of a theoretical model.

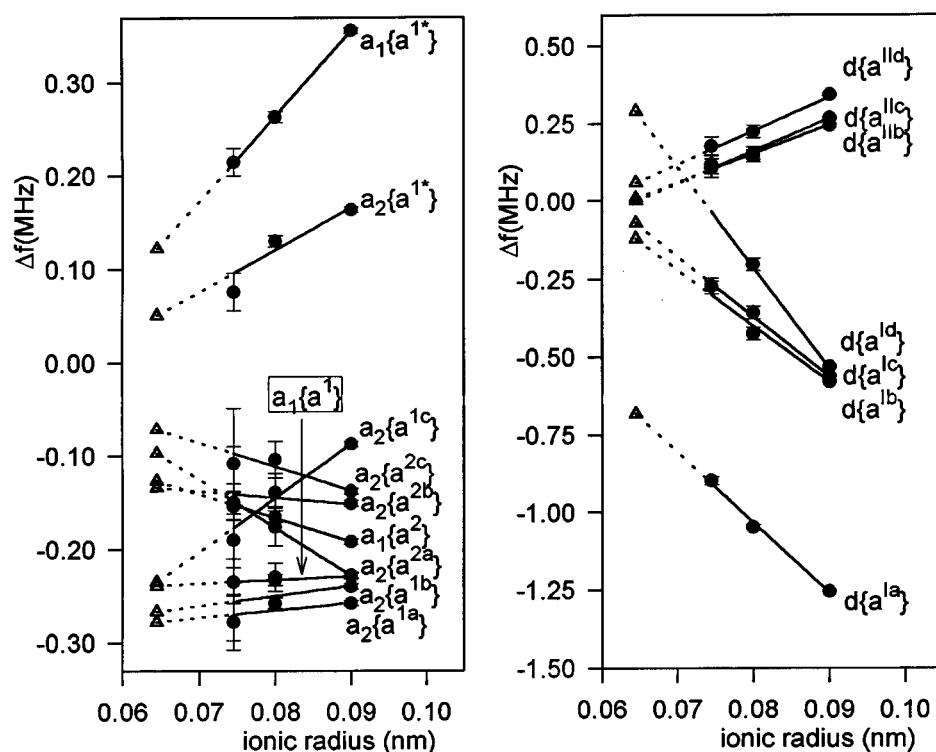


Fig. 7. Dependence of the frequency shift (satellite frequency minus main line frequency) on the ionic radius of the substituent in the *a* site. Circles, experimental values (indicated experimental error); triangles, extrapolated values for the Fe^{3+} ionic radius.

Table 6. Change of the isotropic and anisotropic contributions to the local magnetic field caused by a diamagnetic substitution^A (data extrapolated for the ionic radius of Fe^{3+}) and calculated change in the magnetic dipolar contribution

CEC ^B	ΔI (MHz)	Δq (MHz) ^C	Δr (MHz) ^C	Δs (MHz) ^C	D_1 (MHz) ^D	D_2 (MHz) ^D	D_3 (MHz) ^D
$a\{a^{1*}\}$	-0.069(23)	-0.027(14)	-0.027(14)	-0.027(14)	-0.042	-0.042	-0.042
$a\{a^1\}$	0.255(26)	0.006(28)	-0.003(28)	-0.027(28)	0.042	-0.042	0.042
$a\{a^2\}$	0.107(20)	0.007(31)	0.035(31)	-0.012(31)	0	0	0
$d\{a^1\}$	0.14(10)	0.38(15)	0.034(15)	0.08(15)	0	0.186	0
$a\{d^1\}$	0.889(20)	0.232(30)	-0.022(30)	-0.283(30)	0	-0.186	0

^A Values for the case without substitution minus the values with substitution.

^B Type of crystallographically equivalent configuration of the resonating nucleus and the substituted ion.

^C Change of the non-diagonal elements of the local field anisotropy tensor (experiment).

^D Change of the non-diagonal elements of the dipolar field anisotropy tensor (calculated).

However, to obtain deeper knowledge of the problem and more definite conclusions, a study of other types of YIG substitutions would be desirable. In particular, studies of YIG samples with Ga^{3+} and Al^{3+} ions on the *a* sites and with nontrivalent substitutions of Ge^{4+} or Si^{4+} on the *d* sites would be helpful.

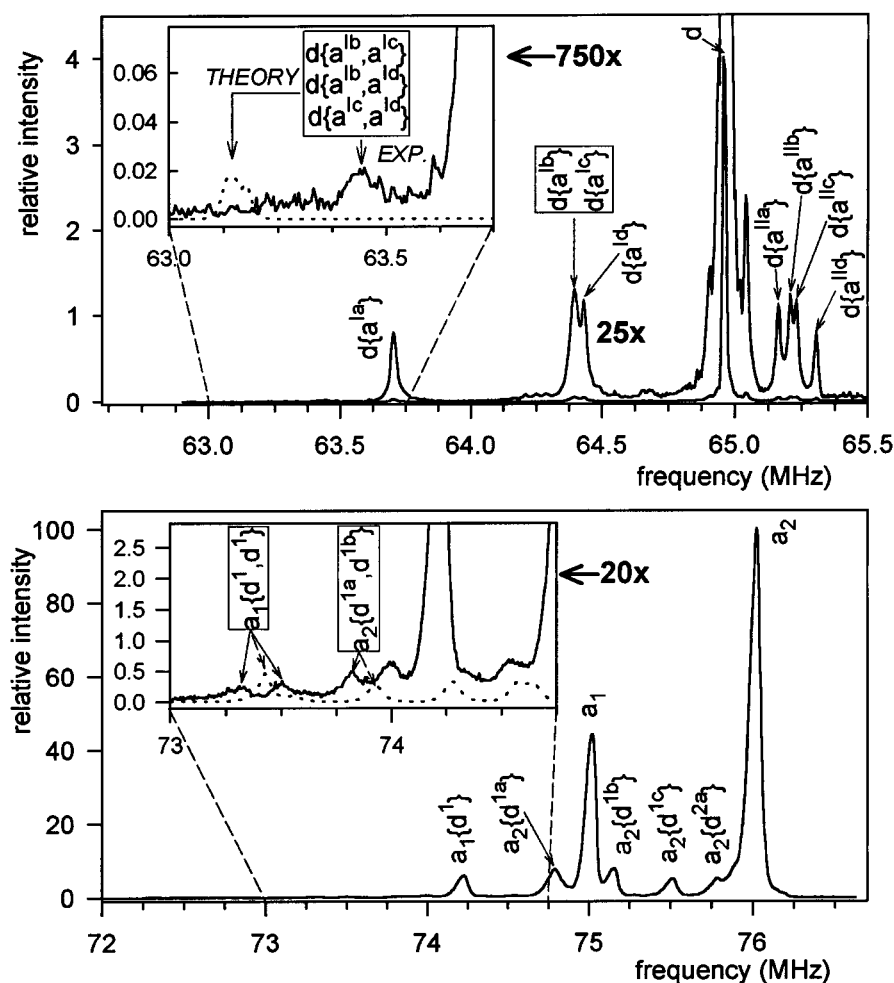


Fig. 8. ^{57}Fe NMR spectrum of YIG with 'antisite' defects in the region of the d site resonance frequency (*top*) and of Ga^{3+} ($x = 0.1$) substituted YIG in the region of the a site resonance frequency (*bottom*) at 4.2 K. Enlarged details (solid curve) show the presence of composite satellites in the experimental spectrum. Dotted curves are the spectra of composite satellites predicted assuming random distribution of the substitution and validity of the superposition rule.

Acknowledgment

This work and its presentation were supported by the Grant Agency of Charles University (grant GAUK 25/97/B) and by the Ministry of Education of the Czech Republic (project PG97297). The DAAD (Deutscher Akademischer Austauschdienst) is also acknowledged for supporting the stay of one of us (J.E.) in KFA Jülich, where some experiments were performed. The authors thank Dr J. Šrámek (Prague), Professor W. Tolksdorf (Ranstadt) and Dr Kimura (Tsukuba, Ibaraki) for providing the samples.

Table 7. Observed composite satellites and scaling factors Φ characterising the deviation of their position from the value predicted by the superposition rule

Composite satellite	Substituent (concentration)	Φ^A
$a_1\{a^1, a^2\}$	In^{3+} ($x = 0.08$)	1.06
$a_1\{a^1, a^2\}$	Sc^{3+} ($x = 0.2$)	1.06
$a_1\{a^1, a^2\}$	Y^{3+} (antisite)	1.08
$a_1\{a^1, a^1, a^2\}$	In^{3+} ($x = 0.08$)	0.99
$a_1\{a^1, a^1, a^2\}$	Sc^{3+} ($x = 0.2$)	1.00
$a_2\{a^{1a}, a^{1b}\}$	Sc^{3+} ($x = 0.2$)	1.00
$a_1\{d^1, d^1\}$	Al^{3+} ($x = 0.1$)	1.05; 0.94 ^B
$a_1\{d^1, d^1\}$	Ga^{3+} ($x = 0.2$)	1.07; 0.95 ^B
$a_2\{d^{1a}, d^{1a}\}$	Al^{3+} ($x = 0.1$)	1.00
$a_2\{d^{1a}, d^{1b}\}$	Ga^{3+} ($x = 0.2$)	1.04
$a_2\{d^{1a}, d^{1b}\}$	Al^{3+} ($x = 0.1$)	0.99
$a_2\{d^{1b}, d^{1c}\}$	Ga^{3+} ($x = 0.2$)	1.06
$d\{a^{Ia}, a^{Ib}\}$	In^{3+} ($x = 0.08$)	1.03
$d\{d^{Ia}, a^{Id}\}$	In^{3+} ($x = 0.08$)	1.00
$d\{a^{Ib}, a^{Ic}\}$	In^{3+} ($x = 0.08$)	1.00
$d\{a^{Ib}, a^{Ic}\} +$ $d\{a^{Ib}, a^{Id}\} +$ $d\{a^{Ic}, a^{Id}\}$	Y^{3+} (antisite)	0.85

^A Defined by formula (7).

^B Observed splitting of the composite satellite.

References

- Brabec, M., English, J., Rotter, M., Novák, P., and Šrámek, J. (1987). *Czech. J. Phys.* B **37**, 86–92.
- English, J., Brabec, M., Novák, P., and Lütgemeier, H. (1985). *J. Mag. Magn. Mater.* **50**, 74.
- English, J., Kohout, J., Novák, P., and Lütgemeier, H. (1994). *IEEE Trans. Magn.* **30**, 972.
- International Tables for X-Ray Crystallography (1952). Kynoch, Birmingham.
- Kohout, J., Štěpánková, H., English, J., Novák, P., and Lütgemeier, H. (1997). *J. Phys. Coll.* IV 7, C1–449.
- Novák, P., English, J., and Lütgemeier, H. (1988). *Phys. Rev. B* **37**, 9712.
- Novák, P., English, J., Štěpánková, H., Kohout, J., Lütgemeier, H., Wagner, K., and Tolksdorf, W. (1995). *Phys. Rev. Lett.* **75**, 545.
- Shannon, R. D. (1976). *Acta Crystallogr. A* **32**, 751.
- Štěpánková, H., Kohout, J., Novák, P., English, J., and Lütgemeier, H. (1998). *J. Mag. Magn. Mater.* **177–81**, 239.
- Tomáš, D., Novák, P., and Štěpánková, H. (1995). *J. Mag. Magn. Mater.* **140–44**, 2133.
- van der Woude, F., and Sawatzky, G. (1971). *Phys. Rev. B* **4**, 3159.
- Wagner, K., Lütgemeier, H., Zinn, W., Novák, P., English, J., Dötsch, H., and Sure, S. (1995). *J. Mag. Magn. Mater.* **140–44**, 2107.
- Winkler, G. (1981). ‘Magnetic Garnets’ (Friedr. Vieweg: Braunschweig).